inventions

MDPI

Article

Research and Development of Trinary Power Cycles

Vladimir Kindra [1,*], Nikolay Rogalev [2], Sergey Osipov [1], Olga Zlyvko [1] and Vladimir Naumov [1]

[1] Department of Innovative Technologies of High-Tech Industries, National Research University "Moscow Power Engineering Institute", 111250 Moscow, Russia; osipovsk@mpei.ru (S.O.); zlyvkoov@mpei.ru (O.Z.); naumovvy@mpei.ru (V.N.)
[2] Department of Thermal Power Plants, National Research University "Moscow Power Engineering Institute", 111250 Moscow, Russia; rogalevnd@mpei.ru
* Correspondence: kindra.vladimir@yandex.ru

Abstract: The most effective and environmentally safe fossil fuel power production facilities are the combined cycle gas turbine (CCGT) ones. Electric efficiency of advanced facilities is up to 58% in Russia and up to 64% abroad. The further improvement of thermal efficiency by increase of the gas turbine inlet temperature (TIT) is limited by performance of heat resistance alloys that are used for the hot gas path components and the cooling system efficiency. An alternative method for the CCGT efficiency improvement is utilization of low potential heat of the heat recovery steam generator (HRSG) exhaust gas in an additional cycle operating on a low-boiling heat carrier. This paper describes a thermodynamic analysis of the transition from binary cycles to trinary ones by integration of the organic Rankine cycle (ORC). A mathematical model of a cooled gas turbine plant (GT) has been developed to carry out calculations of high-temperature energy complexes. Based on the results of mathematical modeling, recommendations were made for the choice of the structure and parameters of the steam turbine cycle, as well as the ORC, to ensure the achievement of the maximum thermal efficiency of trinary plants. It is shown that the transition from a single pressure CCGT to a trinary plant allows the electric power increase from 213.4 MW to 222.7 MW and the net efficiency increase of 2.14%. The trinary power facility has 0.45% higher efficiency than the dual pressure CCGT.

Keywords: Brayton cycle; Rankine cycle; combined cycle power plant; combined cycle gas turbine; regeneration; organic Rankine cycle; trinary power cycle

Citation: Kindra, V.; Rogalev, N.; Osipov, S.; Zlyvko, O.; Naumov, V. Research and Development of Trinary Power Cycles. *Inventions* **2022**, *7*, 56. https://doi.org/10.3390/inventions7030056

Academic Editor: Pierluigi Siano

Received: 26 May 2022
Accepted: 22 June 2022
Published: 4 July 2022

1. Introduction

1.1. Decarbonizing the Power Sector

Currently, world industries experience a stable decarbonizing trend. The reduction of carbon dioxide emission by the power production industry is especially important because of its 39% contribution to emissions in 2017 [1].

The most effective method of emission mitigation in the power production industry is the transition to low-carbon electricity production technologies. These include renewable energy sources (RES), the share of which will continuously grow in the coming decades. Their relevance has only increased in the light of escalating global environmental problems [2,3].

It is worth mentioning that the wide introduction of RES and carbon dioxide capturing systems is limited by the high prices of "green" technology [4,5]. At the same time, today there are alternative ways to reduce anthropogenic greenhouse gas emissions associated with the development of energy-saving technologies with relatively low cost [6–9]. This approach may be applied to the large combined-cycle gas turbines (CCGT) power facilities that are now the most efficient.

1.2. Increasing Efficiency of the Binary Power Cycles

Recently, the development of heat resistant alloys, hot gas path cooling systems and thermal barrier coatings has allowed a working flow temperature increase from 800 to 1650 °C [10,11]. Foreign advanced CCGT facilities have recently reached net efficiency of 63–64% [12,13]. CCGT facilities based on the 9HA02 or M701JAC Gas Turbines (GT) have electric net efficiency above 64% [11,14,15], which is the highest performance among the commercially available gas fuel power production technologies.

Over 100 years of binary technology development, numerous methods for efficiency improvement were proposed and some of them were introduced into practice. Table 1 summarizes the data on CCGT-accessible efficiency improvements and their problems for introduction.

Table 1. Comparison of CCGT facilities efficiency improvement methods.

Improvement Method	Efficiency Increase, %	Method Shortages	Reference
100 °C initial temperature increase	0.9–1.5	Necessity to increase performance of heat-resistant alloys, thermal barrier coatings and turbine hot gas path cooling.	[16,17]
Reheat of combustion products in additional combustors	3.3–3.6	Necessity to install additional combustors, higher cooling flow losses.	[16]
Air compressor inter-cooling	0.7–1.3	Higher compressor cost and reduction of the GT maneuverability due to the higher risk of compressor stall.	[18]
Regeneration of the GT exhausts heat with a regenerator.	1.0–3.5	Necessity to install a regenerator with remarkable mass and dimensions.	[16,18]
Transition from 1P HRSG to 1P + RH	2.25–3.1	Additional HRSG surface and steam pipelines	[19,20]
Transition from 1P HRSG to 2P	1.6–1.8	Additional equipment for the second steam circuit	[19,20]
Transition from 2P HRSG to 2P + RH	0.19–0.5	Additional equipment for the third steam circuit	[19,20]
Transition from 2P HRSG to 3P	0.3–0.5	Additional equipment for the third steam circuit	[19–21]
Transition from 3P HRSG to 3P + RH	0.6–1.09	Additional HRSG surface and steam pipelines	[19–21]

HRSG–heat recovery steam generator; 1P—single-pressure; 2P—dual-pressure; 3P—triple-pressure; RH–reheat.

Most of the known methods provide an electrical net efficiency increase of 0.6–3.6%. Their application usually requires capital investment increase, and sometimes power facility maneuverability and reliability are compromised. Therefore, the use of various methods or their combinations is not always justified from an economic point of view.

The main method for CCGT efficiency improvement is the increase of GT cycle initial temperature. A 100 °C gas turbine inlet temperature (TIT) increase leads to a power unit efficiency increase of 0.9–1.5% [16,17]. It is worth mentioning that the available nickel alloys can operate at temperatures below 900 °C, and the cooling systems efficiencies are near to their limits [22]. In this regard, further increase in the net electrical efficiency of CCGTs by increasing the initial temperature of the gas turbine is troublesome.

Reduction of the GT exhausts heat recovery losses is an alternative approach to CCGT efficiency improvement. Traditionally, the exhaust gases at the exhaust of a gas turbine are sent to a waste heat boiler (HRSG), which generates water vapor to power the steam turbine. The HRSG may be of a single-, dual-, or triple-pressure type. The larger amount of HRSG pressure improves the recovery of GT exhaust heat and thus increases useful electricity production. It is also possible to use steam reheat to improve energy efficiency. Specific features of the CCGT steam cycles are due to the properties of the heat source that is the exhaust gas flow. Efficient heat transfer combined with the maximal heat potential is reached at the minimal surface of the figure between the heating and heated flows in Qt diagram of HRSG. Increase in pressure used and introduction of the reheat allows for reduction of heat potential losses. This limit is caused by the necessity to evaporate the heat carrier that is maintained at a constant temperature and produces maximal heat potential losses in a HRSG.

The introduction of the additional pressure in HRSG with lower parameters allows for efficient recovery of additional heat [23,24]. The maximum amount of heat recovered in this case is limited by the minimal exhaust temperature that is determined by the steam saturation condition and the low temperature corrosion of tail heating surfaces in the presence of sulfur in the fuel, and the perfection of the HRSG.

Therefore, one of the ways to increase the efficiency of steam–gas plants may be the creation of circuits with a low-boiling coolant, which will make it possible to realize the low-temperature potential of heating gases.

Galashov and Tsibulsky [25] considered the use of ammonia, butane, pentane, R236fa, and R245fa for utilizing the heat of condensate after the condensate pump and the latent heat of steam condensation after the steam turbine of a CCGT in an ORC with a regenerator. When using gas turbine NK-36ST and a single-pressure HRSG with initial parameters of 16 MPa and 440 °C, the use of ORC allows for efficiency higher than 60% at a condensing temperature in a low-potential cycle of less than 0 °C. The most effective is the use of pentane in ORC, followed by butane, R245fa, R236fa, and ammonia. The same authors in [26] considered CCGT using 9HA.02 with low-potential cycle using pentane, butane, R365mfc, RC318, R236ea, R236fa, R123, R245ca, and R245fa. It was determined that the most promising were pentane and R365mfc. The use of low-potential cycles in CCGT with reheat with SGT5–8000H was considered in [27]. Butane was used as a low-boiling fluid.

Utilization of low-potential energy of gas turbine exhaust gases was considered by Bălănescu and Homutescua [28]. When using the gas turbine Orenda OGT1500, the gas temperature at the HRSG exhaust is 188 °C, which makes the use of ORC justified. The net electrical efficiency was 45.47% when using R134a in ORC and 45.56% when using R123, which is 1.1 and 1.19% higher than the efficiency of the prototype.

The unconventional approach was studied by Gafurov et al. [29]. The trinary cycle used NK-37 gas turbine as a heat source for two low-temperature cycles. The first one used single-pressure HRSG with benzol and the second one utilized the heat of stream from turbine and latent heat in condenser. The second cycle uses butane and has a regeneration. The use of trinary cycle allowed increase in efficiency of up to 62.6%.

Therefore, one of the methods for CCGT efficiency improvements may be creation of low-boiling heat carrier cycle that will allow utilization of the low-temperature heat of flue gases.

1.3. Binary Power Cycles in Russia

In the USSR, studies of combined thermodynamic cycles began in the 1930s of the 20th century, and practical implementation began in the 1960s. Despite this long investigation and development period, the combined cycle facilities were not widely used.

Currently in Russia, the CCGT direction is one of the power industry priorities. Transition to the carbon dioxide emission market system will result in a competition between the electric power production companies. Therefore, the main power production companies will be interested in development of highly efficient facilities.

In Russia, there are at present 68 power production companies which have 98 CCGT facilities with a total power of 25.7 GWt. The General Scheme for Power Production Facilities Locations by 2035 includes startup of 81 more facilities with 23.0 GW total power at 37 power generation companies. Therefore, the plan is to double the CCGT power in the oncoming decade. The domestic power industry is mostly equipped with CCGT facilities of 200–250 MW and 400–450 MW capacity (Figure 1a). The most common are the single-block and double-block unit; the triple-block facilities are rare. More than 70% of Heat Recovery boilers (HRSG) are of twin-flow type [30].

Most of the Russian CCGT facilities have electrical net efficiency of 50–59%, which is lower than the 63–64% of the advanced foreign ones. This is mostly due to the remarkably lower level of the domestic GT technology. The CCGT facilities with about 39% of installed power are equipped with GT with TIT, which is the key parameter for the cycle efficiency below 1100 °C (Figure 1b). High power GT with TIT above 1500 °C are absent. Large

foreign power consortiums are developing GT with TIT about 1700 °C, so the prospects for domestic GT efficiency improvement are remarkable.

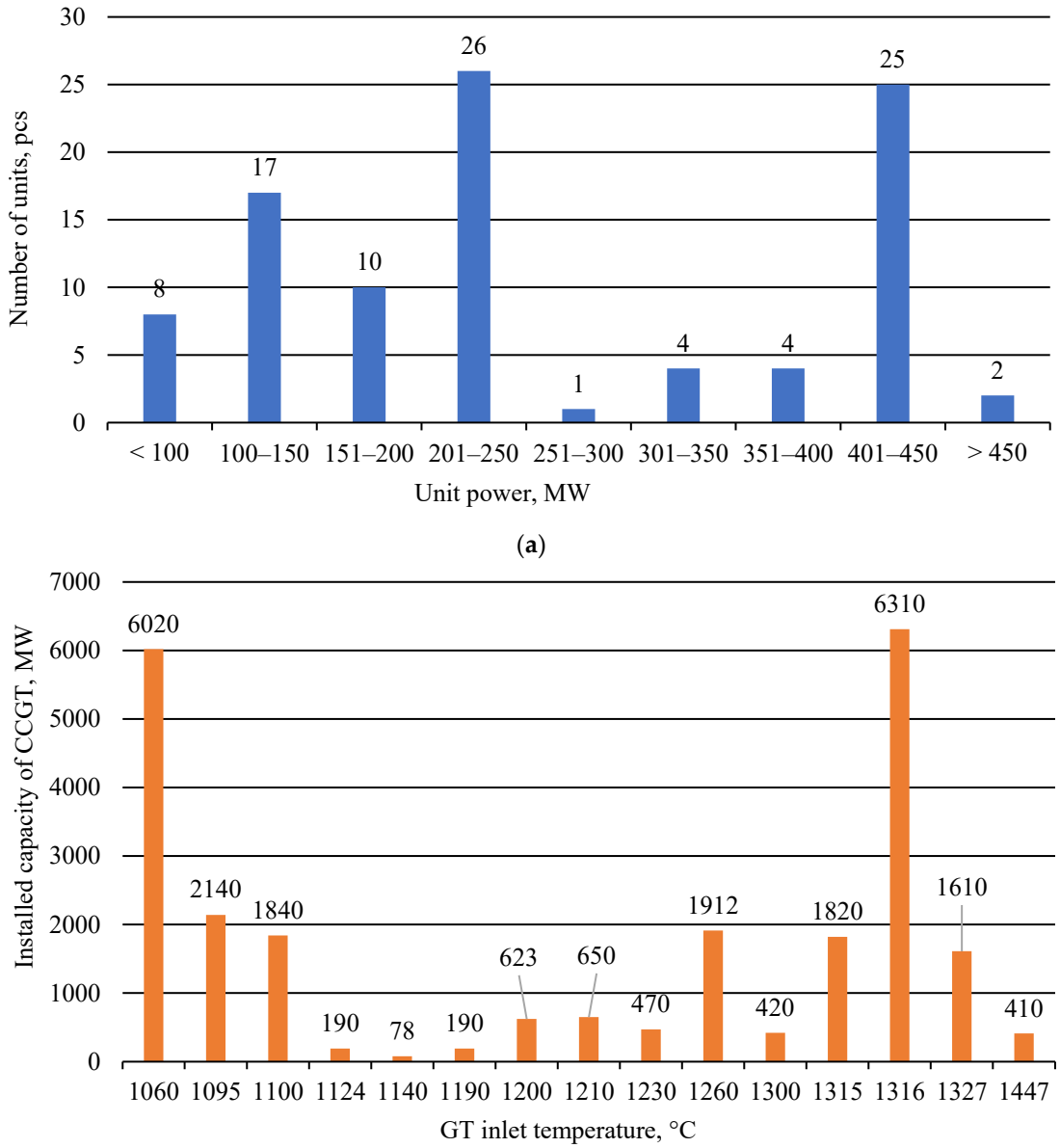

Figure 1. Statistical data on the CCGT facilities technical level in Russia: (**a**) distribution of the number of CCGTs depending on the installed capacity, (**b**) distribution of installed CCGT capacities depending on the gas TIT.

Reduction of this gap will require considerable time and investments. The CCGT power production efficiency and environmental safety improvement without excessive time and financial losses requires assessments of reasonable improvement directions for operational and prospective facilities.

It is possible to achieve a significant improvement in CCGT facility efficiency with low-boiling heat utilization cycle via introduction of steam turbine unit (STU) heat regeneration. This technical solution has a complex effect since its use not only leads to a significant reduction in losses in the condenser of a STU, but also allows higher heat carrier temperature in the low-temperature cycle due to the higher flue gas temperature related to the higher feed water temperature.

The purpose of this research is developing a thermodynamic analysis of thermal circuits of power plants operating on trinary cycles, as well as providing recommendations for their application in order to increase the efficiency of electricity generation.

2. Materials and Methods

As the flue gas source, the GTE-160 was chosen since it is the main GT manufactured in Russia. The studies were based on computer models of a cooled GT and an STU single-pressure facility with a regeneration system. The transition to a trinary cycle power plant was conduct by using the GT flue gas heat for power production in a low-potential cycle. A transition to a dual-pressure HRSG was considered for the comparison.

2.1. Single-Pressure CCGTs

Figure 2 shows the single-pressure CCGT power plant scheme. Air enters the air compressor (AC) where it is compressed. A small part of the compressed air is sent to cooling of the GT hot gas path elements. The main part of the air enters the combustion chamber (CC). Fuel is compressed in the fuel compressor (FC) and supplied to CC. Fuel combustion raises temperature of the working fluid that further enters the GT inlet. The potential energy of high-temperature gas is spent for the GT rotor rotation. The rotor is mounted on a shaft together with a first electricity generator (EG1). The gas turbine exhaust gas enters the heat recovery steam generator that produces steam for an STU. In the HRSG, gas subsequently passes heating surfaces of the steam superheater (SH), evaporator (EV), economizer (EC), and water heater (WH). The HRSG exit gas is released into atmosphere. Steam produced in the SH is sent to the STU high pressure turbine (HPT). After the steam has produced useful work, it is partly sent to the deaerator. Most of the steam is sent to the STU low pressure turbine (LPT), where its heat drops and enters the condenser. The resulting condensate is sent to the condensate pump (CP) and to the water heater. The condensate heater inlet temperature is kept constant by a recirculation pump (RP). The pre-heated water is sent to Deaerator (D), heated up to the saturation point by the steam, purified from harmful non-condensing gases, and supplied to the feed water pump (FWP) driven by an electric motor. The high-pressure water is sent from the FWP to the economizer, where it is heated close to the saturation temperature. Then water is sent to the natural circulation evaporator drum. Saturated water from the drum passes the evaporator surfaces and part of the it is converted into steam. Then the water-steam mixture enters the drum where the steam is separated. The saturated steam from the evaporator drum enters the steam superheater. The second electricity generator (EG2) is mounted on the steam turbine shaft and produces electricity.

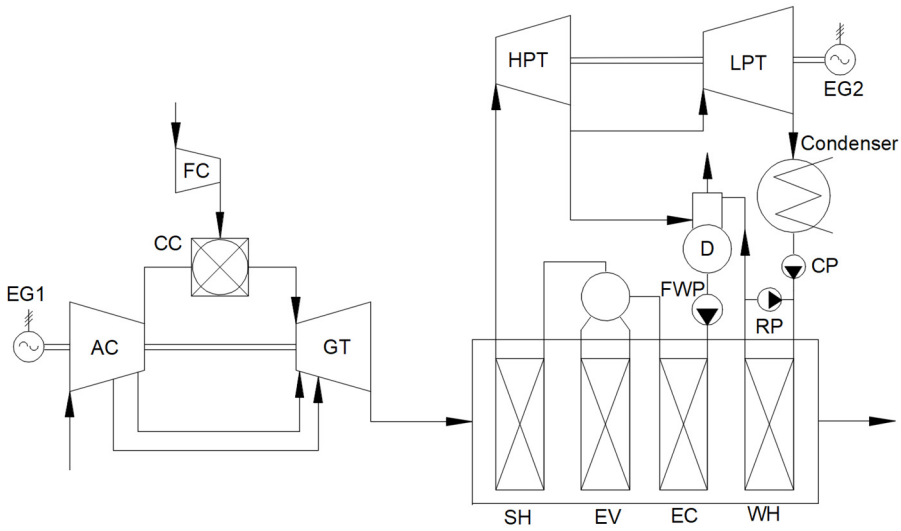

Figure 2. Single-pressure CCGT power plant with a cooled GT.

Influences of the feed water temperature and the regenerative STU extraction upon the trinary cycle facility parameters were studied in a single-pressure power plant with a low-pressure regeneration system (Figure 3). Application of two and three low pressure heaters (LPH) was also considered.

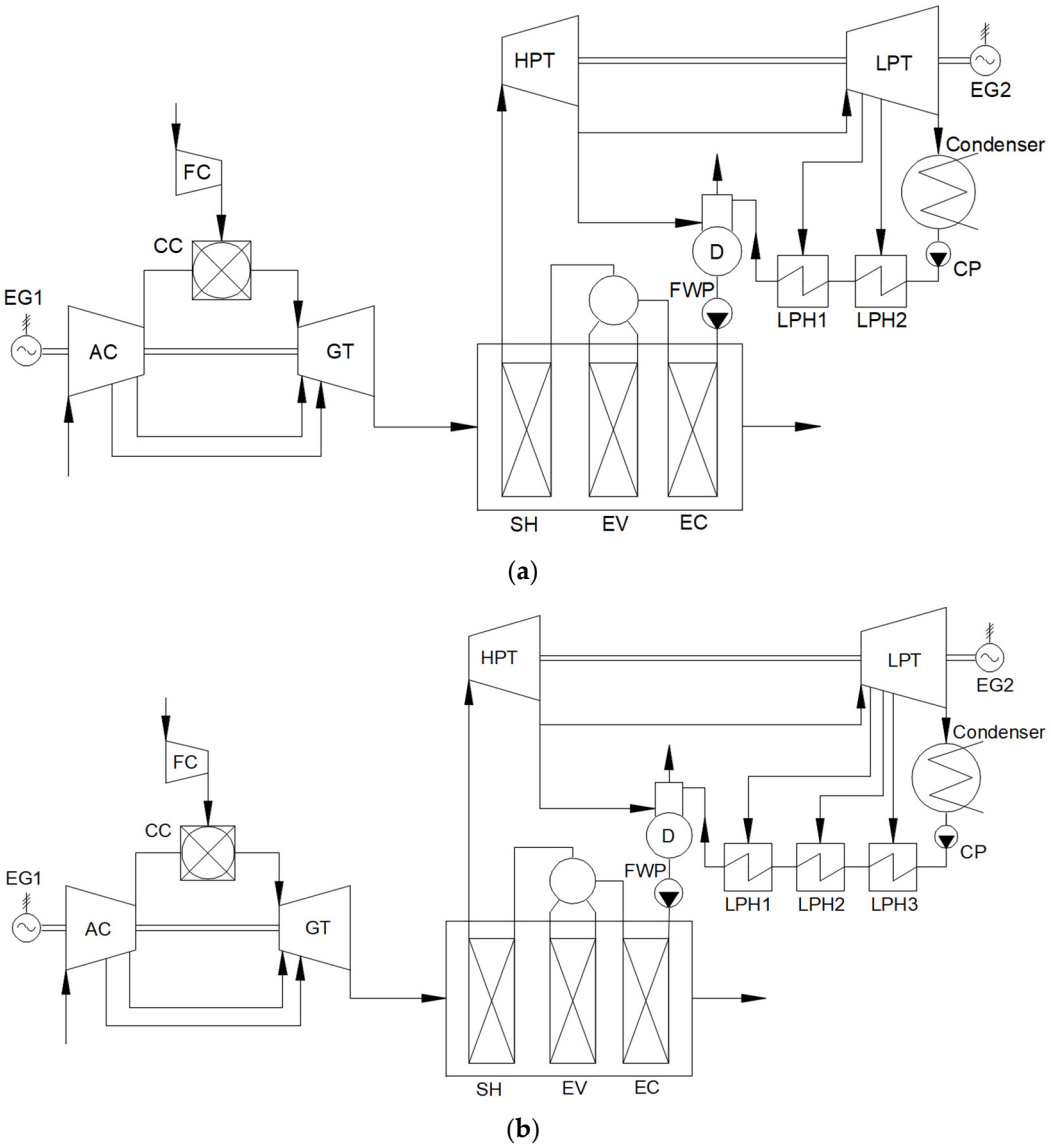

Figure 3. Single-pressure CCGT power plants with a cooled GT and a low-pressure regeneration system: (**a**) two LPHs, (**b**) three LPHs.

This facility differs from the one in Figure 2 by the condensate heating at the deaerator inlet in the low-pressure regeneration system. Because of this, there is no water heater in the heat recovery steam generator. The CP supplies water to the inlet of a series-connected group of low-pressure heaters, in each of which the condensate temperature increases by the same amount. All LPHs are of surface type with the drainage to condenser. Water is heated in the LPH by the steam extraction from the LPT. All other processes in the facility are equal to the single-pressure CCGT ones shown in Figure 2.

2.2. Dual-Pressure CCGT

There are dual-pressure power plants based on the GTE-160; therefore, a heat flow scheme of a dual-pressure CCGT was also developed (Figure 4). This plant will be compared with the developed trinary cycle one. The dual-pressure trinary differs from the single-

pressure one by the application of high- and low-pressure feed pumps, superheaters, evaporator, drums, and economizers.

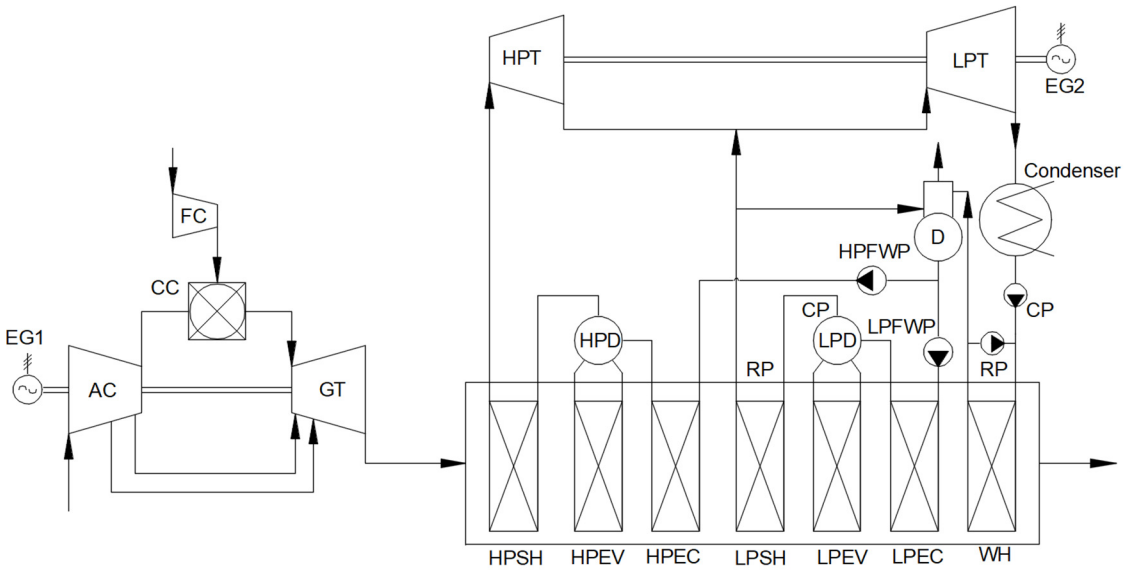

Figure 4. Dual-pressure CCGT power plant with a cooled GT.

Table 2 summarizes input data for the CCGT power plants modeling [31].

Table 2. CCGT analysis input data.

Parameter	Value
GT flue gas massflow, kg/s	509
GT initial temperature, °C	1060
GT pressure ratio	10.9
Exhaust gas temperature, °C	523.3
Fuel compressor internal relative efficiency, %	88
Steam turbine internal relative efficiency, %	90
Superheater hot end temperature difference, °C	20
HRSG maximum exit steam temperature, °C	560
Evaporator cold end temperature difference, °C	10
Economizer outlet water subcooling, °C	10
Deaerator inlet water subcooling, °C	10
Condenser temperature difference, °C	5
Cooling water temperature after the condenser, °C	25
Minimal heat carrier temperature at the HRSG inlet, °C	60
Minimal flue gas temperature at the HRSG exit, °C	80
Deaerator pressure, MPa	0.12
Pressure loss in superheater, %	5
Excess of pressure in deaerator extraction relative to deaerator pressure, %	40
Pressure loss between the condensate pump and deaerator, %	40
Internal efficiency of feed water and condensate pumps, %	85
Vapor fraction at the steam turbine exit, %	90
Mechanical efficiency, %	99
Electric motor and power generator efficiencies, %	99

2.3. Organic Rankine Cycles

Utilization of low-potential heat was assessed in an organic Rankine cycle unit (ORC). The Figure 5a plant corresponds to a facility that can operate at different working fluid pressures, sub- and supercritical. Figure 5b describes a Rankine cycle with its organic turbine operating a superheated steam at sub-critical pressure. The working fluid expands in an organic turbine (process 1–2). Then, the fluid enters the condenser where it passes

cooling (process 2–2″) and condensing (process 2″–3). The produced condensate is sent to the Organic Pump (OP) (process 3–4) and to the heat source for heating (process 4–1).

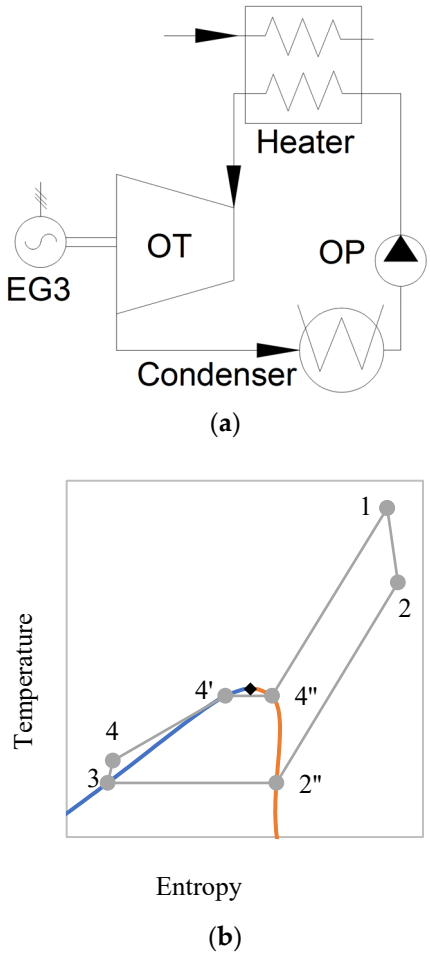

Figure 5. Organic Rankine cycle: (**a**) plant, (**b**) subcritical pressure cycle with superheated steam.

The advantage of Rankine-cycle-operating saturated steam is the possibility to reach maximal thermal efficiency at a constant heat source temperature and constant underheating degree. Its drawback is the risk of moisture formation in the expansion process for a number of low-boiling working fluids, in which the saturation curve moves towards an increase in entropy with decreasing temperature (R14 and others). At a remarkable moisture content, the turbine last stages will have shorter operating life due to the erosion wear.

The working fluid heating above the saturation parameters reduces the risk of moisture formation in turbine flowpath. An excessive superheating may cause exit working fluid overheating, and this increases the mean integral heat removal temperature. This factor may reduce the cycle thermal efficiency.

Figure 6 shows a cycle with the regeneration used for reduction of the cold source losses. Unlike the simpler cycle (Figure 5) here the organic turbine flow enters the regenerator and cools down (process 2–5) while heating the flow downstream the organic pump (process 4–6).

Table 3 summarizes the ORC analysis fixed input data. The main variable parameter was the initial pressure. The organic working fluids chosen were the following: R41, R22, R134a, R236ea, and R124 [32].

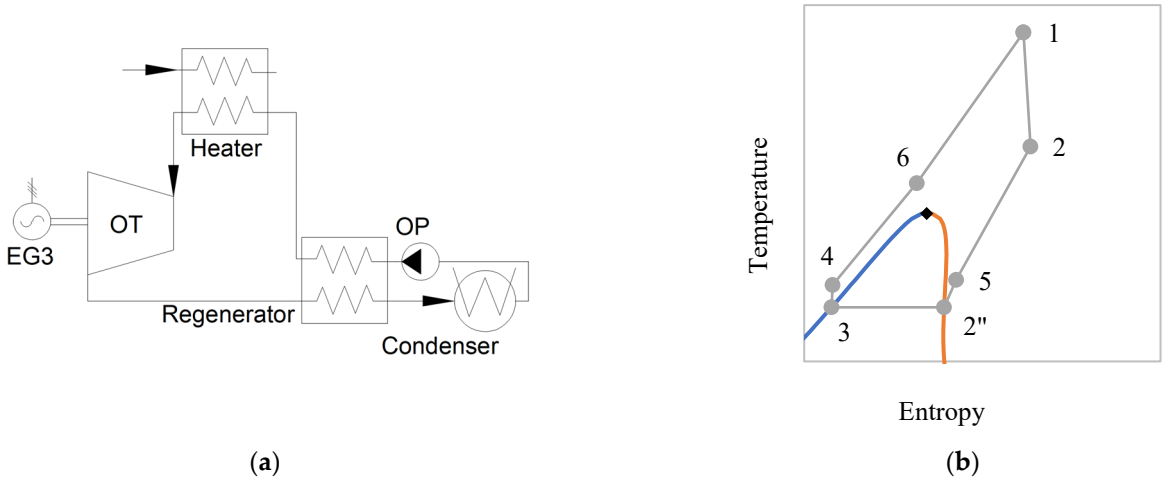

(**a**) (**b**)

Figure 6. Organic Rankine cycle with regeneration: (**a**) plant, (**b**) supercritical cycle.

Table 3. Organic Rankine cycle analysis input data.

Parameter	Value
Minimal cycle temperature, °C	30
Minimal regenerator temperature difference, °C	5
Pump internal relative efficiency, %	85
Turbine internal relative efficiency, %	85
Power generator and electric motor efficiency, %	99
Mechanical efficiency, %	99

2.4. Trinary Cycles

When the low potential heat of CCGT exhaust gas is utilized in an ORC, it is possible to form a trinary power plant with and without low-pressure regeneration in an STU (Figure 7). The trinary power facility consists of a GT, STU, and low-potential ORC plants.

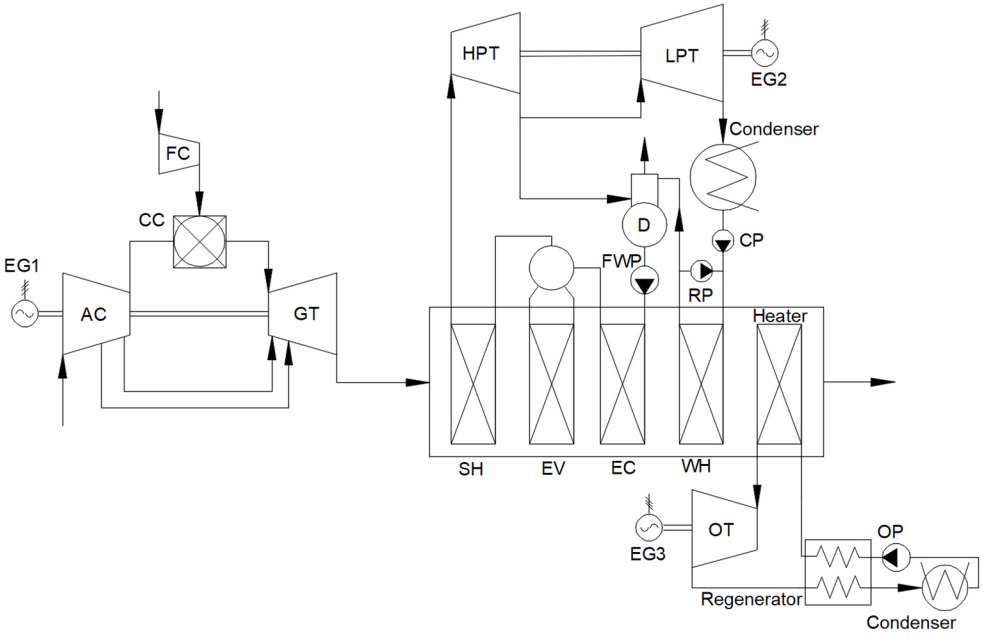

(**a**)

Figure 7. *Cont.*

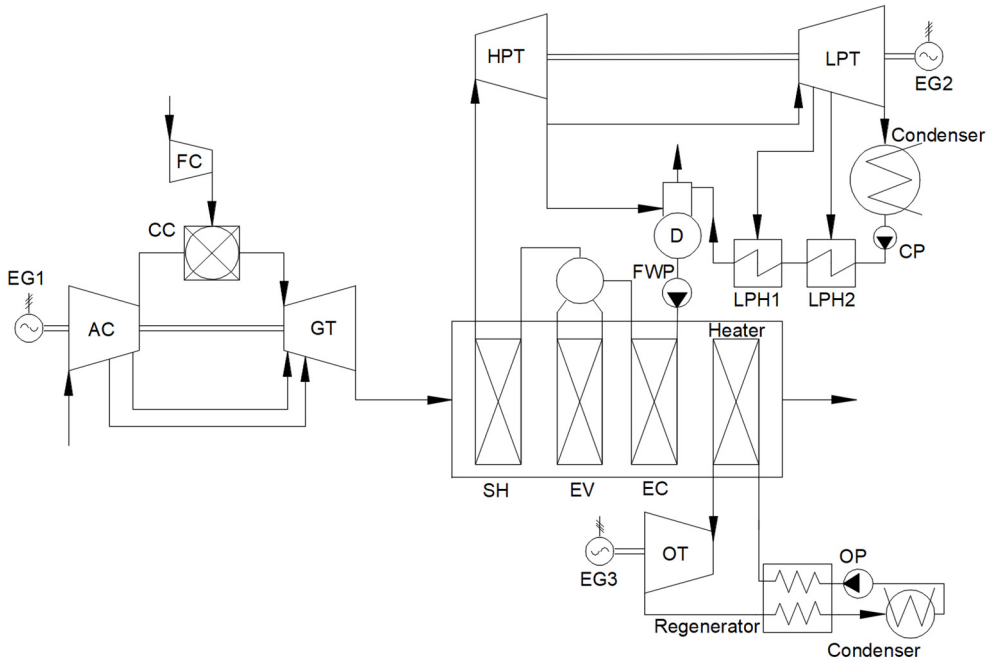

(**b**)

Figure 7. Trinary power cycles: (**a**) with a single-pressure CCGT, (**b**) with a single-pressure CCGT and low-pressure regeneration in STU.

The effect of transition to the trinary cycles may be assessed with mathematical models of binary and trinary power plants equipment. A CCGT facility consists of a GT and a STU that receives heat from a heat recovery steam generator. Contents and parameters of the GT exhaust gas flow may be obtained from a cooled GT model. This model will then be used to create the CCGT power plant model. Transition to the trinary cycles also needs the creation of ORC model. All models used were created in the Aspen Plus V10 computer program [33]. The working fluid thermo-physical properties were taken from the NIST Reference Fluid Thermodynamic and Transport Properties Database v10 (REFPROP), which is known for its high accuracy [34].

2.5. Aircooled Gas Turbine Model

First, a mathematical model of a cooled gas turbine was developed. The coolant flow calculation was based on available data on energy characteristics of the existing units. This approach makes it possible to obtain a model of a cooled GT with characteristics close to those of the existing ones without the need for design of the flow path and the cooling system.

To create the same simulation conditions, the following parameters were fixed (Table 4): the ratio of coolant flow into each of the GT compartments and the relative internal efficiencies of the compressor and turbine.

The cooled GT mathematical model (Figure 8) was created on the basis of Aspen Plus computer program [33] that allows for simulation of complicated power plants. The model consists of the following elements. The air compressor model is split into three parts, AC1, AC2, and AC3, which are related to the coolant bleeding BLEED1 and BLEED2 [35]. Combustion chamber (CC) is supplied with compressor exit (AIR) and fuel (CH4) flows. Methane was used as fuel.

Table 4. GT modeling input data.

Parameter	Value
Ambient air temperature, °C	15
Ambient air pressure, KPa	101.3
Fuel	CH_4 (methane)
Compressor internal relative efficiency, %	88
Turbine internal relative efficiency, %	89
Combustion chamber pressure loss, %	3
Coolant flow distribution (COOLING1:COOLING2), %:%	70:30
Mechanical and power generator efficiency, %	99

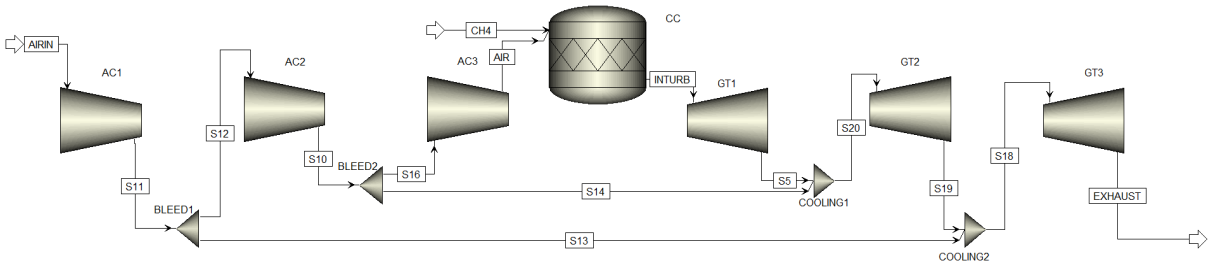

Figure 8. Cooled gas turbine model.

In the combustion chamber, fuel is burned in a stoichiometric ratio according to the reaction:

$$CH_4 + 2O_2 \rightarrow 2H_2O + CO_2 \quad (1)$$

The fuel pressure is assumed to be 30% higher than the pressure of the air entering the CC. After the combustion chamber, the gas enters the turbine where the power is produced. Then the gas turbine is split into three parts, GT1, GT2, and GT3. The cooling flows ratio COOLING1 to COOLING2 is assumed to be 70:30 [36]. Pressures between the turbine parts were assumed from the condition of using four stages. The coolant was supplied after the first and second stages with pressures at the outlet selected so that the heat drop was divided into four equal parts.

The developed model of a cooled GT has the following assumptions:

- coolant bleeding from the compressor does not depend upon the cooling system efficiency (this is determined by the Aspen Plus capabilities),
- the model does not take into account the cooling air injection after each vane or blade row,
- pure methane combustion is stoichiometric,
- compressor and turbine relative internal efficiencies and the combustor losses are assumed constant for all GTs.

These assumptions are not significant for the generalized studies of the cooling air flow influence upon the GT performance and verification of the model accuracy.

Russian companies have experience in creation of powerful power production gas turbines [37]. In particular, the gas turbine unit GTE-110 [38] has been developed and is being tested. But the main manufacturers of large power production GTs are the following companies: Siemens energy (Munich, Germany), General Electric–GE (Boston, MA, USA), Alstom Power (Saint-Ouen, France), Mitsubishi Heavy Industries-MHI (Tokyo, Japan), Ansaldo Energia (Genoa, Italy) [11].

The total coolant flow was verified in a range assumed for each of the GTs. The study goal was to reach the coolant flow close to that one in the actual GT. The study of gas turbines of different generations (Table 5) makes it possible to compare installations with different initial temperatures and compression ratios, but also cooling systems, alloys, and other characteristics. Thus, the generalization of GT characteristics with different design features is a necessary assumption in the development of a mathematical model that takes into account the initial parameters.

Table 5. Nominal performance of gas turbines under study.

Manufacturer	Model	N_e, MW	TIT, °C	PR	t_{exh}, °C	G_{exh}, kg/s	Efficiency, %	Reference
Mitsubishi Heavy Industries	701DA	144.09	1250	14	542	453	34.8	[15]
	701G	334	1410	21	587	755	39.5	
	701F	385	1500	21	630	748	41.9	
	701J	478	1600	23	630	896	42.3	
	701JAC1	448	1650	25	663	765	44	
	701JAC2	574	1650	25	646	1024	43.4	
	701F4	312.1	1400	18	590	703	39.3	[31]
	701F	270.3	1350	17	586	664	38.2	[39]
	701G	334	1410	21	587	750	39.5	
Siemens	4000F	265	1315	17	584	656	38.5	
	8000H	340	1500	19.2	625	820	39	
	V64.3	60	1120	15.6	534	187	35.2	[31]
	V94.3	200	1120	15.6	534	605	35.7	
	2000E (V94.2) /GTE-160	153	1060	10.9	537	509	33.9	
	9001FA	255.6	1288	15.4	609	624	36.5	[39]
	9G	282	1430	23	583	700	39.5	
Alstom Power	GT13E2	164.3	1100	15.4	525	623	35.7	
JSC NPO Saturn	GTE-110	114.5	1210	14.7	517	362	36	[31]

N_e—electric power; PR—pressure ratio; t_{exh}—exhaust temperature; G_{exh}—exhaust mass flow.

The wide ranges of the considered GT pressure ratio and turbine inlet temperature allows creation of the dependence shown in Figure 9. This dependence can be expressed by the equation:

$$\pi_k = 0.0198 \cdot t_0 - 8.35, \quad (2)$$

where t_0—turbine inlet temperature, °C; π_k—air compressor pressure ratio.

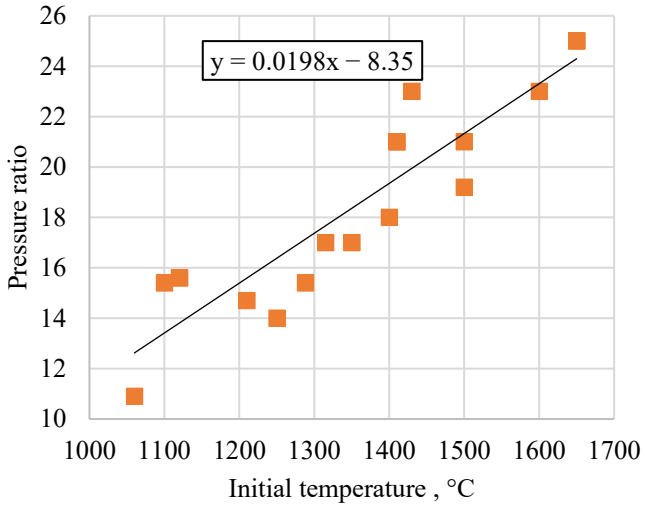

Figure 9. Dependence of pressure ratio on initial GT temperature.

For each GT, analysis was conducted at different coolant massflow values. Then, using the interpolation of available characteristics (Table 5) and modeling results, the possible coolant flow rates (Figure 10) were determined for various controlled values (efficiency, gas turbine power, flue gas temperature).

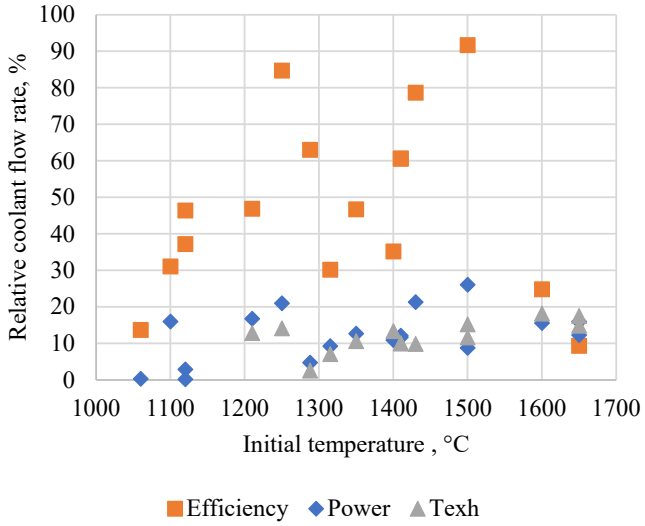

Figure 10. Relative coolant flow rate dependence on initial GT temperature biased on the efficiency, power, and exhaust gas temperature.

Figure 10 shows overestimated and remarkable differences in relative coolant mass-flows calculated from the GT efficiency against the rate calculated from other parameters. This is because of the GT efficiency calculation algorithm, which is based on the elements' efficiency, flowpath losses, and many other factors that are difficult or impossible to assess on the basis of published data. Therefore, in further calculations, the relative coolant flow was calculated by the criteria of equality of power output and exhaust gas temperature. According to the obtained values, it can be seen that the dependence does not have a clearly defined character, however, there is a positive correlation; therefore, a linear approximation was chosen.

The obtained relations of coolant massflow with the initial temperature and pressure ratio allow a 3D linear approximation. However, since the TIT and pressure ratio are related (Figure 9) it is reasonable to form the coolant flow dependence from the initial temperature alone:

$$\psi_{ox\pi} = 0.0268 \cdot t_0 - 25.98, \quad (3)$$

This dependence is based on a wide set of GTs with pressure ratios in range of 10.9–25 and TIT of 1060–1650 °C. Figure 11 shows results of the Equation (3) calculation.

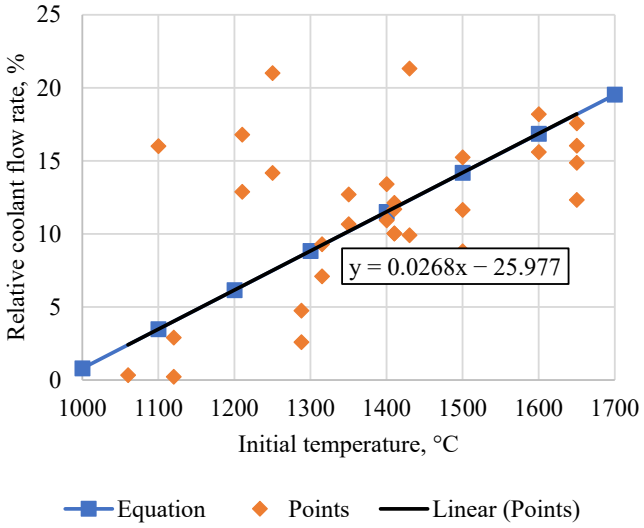

Figure 11. Relative coolant flow rate dependence from turbine initial temperature.

2.6. CCGT Models

The developed cooled GT model was used for modeling of binary power plants. For example, Figure 12 shows a single-pressure GTCC model. The GT analysis was conducted with the input data listed in Table 2 and according to the Equation (3). The feed water pump exit pressure was tuned for the steam vapor fraction of 90% at the turbine exit. This fraction is higher than the usual published value, but the actual turbine efficiency is different in different compartments and drops down during the humid steam operation. Therefore, the real humidity at the ST exit will be lower. The primary steam flow calculation satisfied the superheater and evaporator heat balances together with temperature differences along the HRSG. When the heat recovery steam generator exit gas temperature was below 80 °C, the primary steam flow was selected to ensure its minimal value.

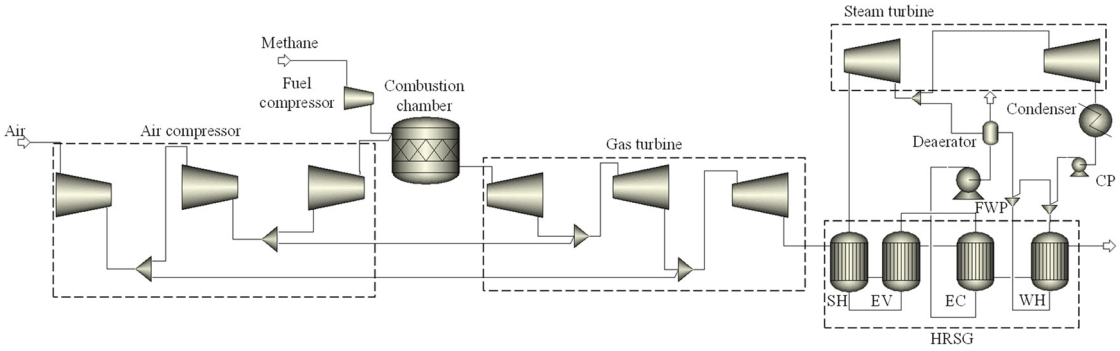

Figure 12. Mathematical model of a single-pressure CCGT with cooled GT.

Input data for modeling of the CCGT with regeneration in the STU were taken from Table 2. The regeneration system was calculated with the subcooling of 5 °C and pressure losses in the pipelines between turbine and LPH of 5%. The condensate heating was equally distributed between the available LPHs. The analysis was done for three levels of feeding water temperature that correspond to standard deaerator pressures (0.7, 0.3, and 0.12 MPa).

During the dual-pressure CCGT modeling the feed water pressure was tuned in such a way that the turbine exit steam vapor fraction was equal to 90%. The second pressure was calculated om the operating conditions of the deaerator.

2.7. ORC Model

The last element for the trinary power plant computer model is the low-potential cycle model. The ORC analysis input data corresponded to Table 3. The turbine inlet temperature was determined by the temperature difference at the heater hot end of 20 °C and the exhaust gas temperature of 80 °C. When the minimal temperature difference in the heater was below 10 °C, the organic fluid flow was increased as to satisfy this condition. The plant model created in the Aspen Plus computer program is shown in Figure 13.

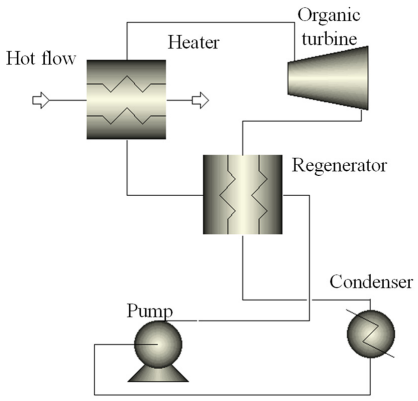

Figure 13. ORC mathematical model.

3. Results and Discussion

On the basis of these simulation models, parameters of the basic binary power plants were calculated. In all considered facilities, the GTE-160 was used for the basic high temperature cycle; therefore, at first, the parameters of its operation were calculated. Next were calculated the single- and dual-pressure CCGT power units. These facilities are basic and represent traditional utilization cycles, constructed in Russia. Then, the power unit parameters necessary to evaluate the transition to trinary cycles were calculated. First, the CCGT facility parameters were calculated for a regeneration system that allows higher HRSG gas exhaust temperature and higher STU efficiency. This will reduce the binary facility efficiency but may have a positive effect in a trinary cycle. Further, parameters of low potential utilization cycles were calculated, and a transition to trinary cycles was assessed.

3.1. Traditional CCGTs

Table 6 summarizes the GT calculation results. The obtained characteristics are near to the nominal values (Table 5). The calculated single-pressure CCGT net power and efficiency were 213.4 MW and 49.2%, respectively.

Table 6. Calculated GTE-160 operation parameters.

Parameter	Value
Turbine initial temperature, °C	1060
Pressure ratio	10.9
GT flue gas massflow, kg/s	509
GT net power, MW	143.5
GT net efficiency, %	33.1
Exhaust gas temperature, °C	523.3
Exhaust gas composition, mol %:	
N_2	77.98
O_2	12.26
CO_2	3.05
Ar	0.66
H_2O	6.05

The developed trinary CCGT facility parameters were compared with the traditional efficiency improvement methods. Figure 14a shows the dependence of exhaust gas temperature from the feed water temperature or the deaerator pressure. The smaller deaerator temperature and steam pressure led to higher utilization of the flue gas heat. At all feed water temperatures, the dual-pressure CCGT power unit net efficiency is higher than the single-pressure one (Figure 14b).

The dual-pressure CCGT has a maximum net efficiency of 50.9% which is rather near to the dual-pressure double-block PGU-450 efficiency of 50.5% [40]. The transition to a dual-pressure CCGT when using GTE-160 leads to an increase in net efficiency of 1.1–1.7%, which coincides with the data obtained as a result of a literature review (Table 1). Thus, the developed model allows for adequate assessment of traditional CCGT facilities parameters.

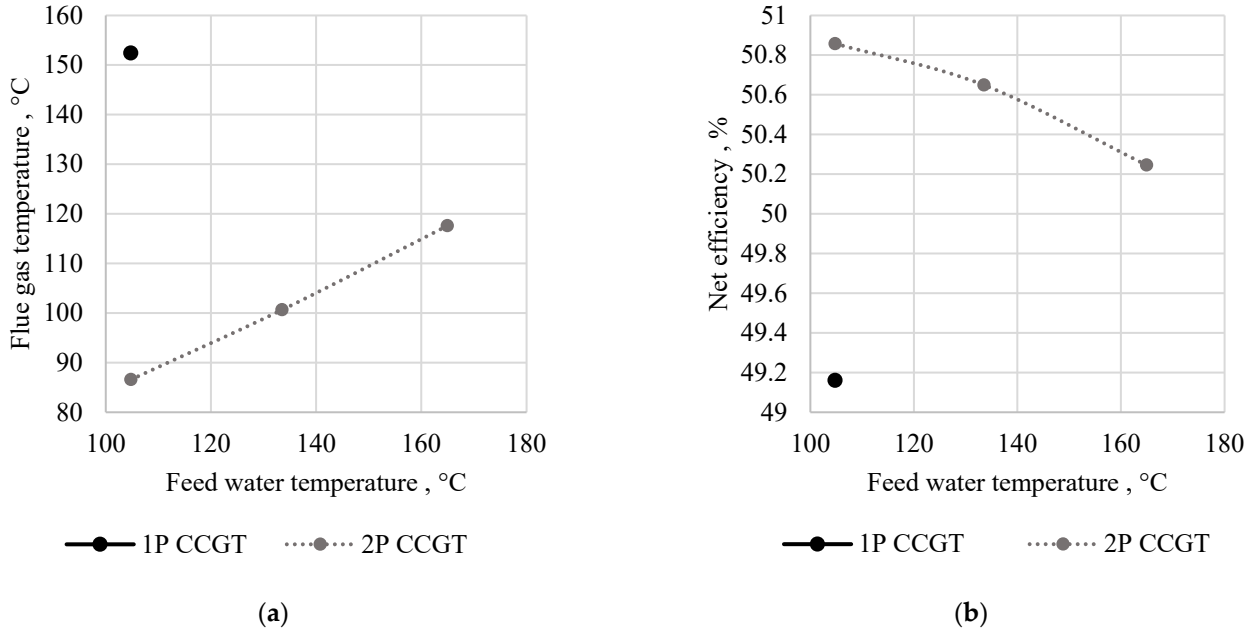

Figure 14. Dependence of the dual-pressure CCGT parameters on the feed water temperature: (**a**) flue gas temperature, (**b**) net efficiency.

3.2. Single-Pressure CCGT with Regenertion

Further, various options for using the regeneration system in STU were considered, which may be effective in the transition to a trinary plant. Figure 15a shows gas temperature after the HRSG in a single-pressure CCGT with regeneration with application of two and three LPHs and without regeneration. As expected, the CCGT without regeneration shows the smallest flue gas temperature. In a CCGT with regeneration, the exit gas temperature increases by 30–60 °C, which is due to the absence of a water heater and the higher temperature of the water supplied to the HRSG, which reduces its thermal power.

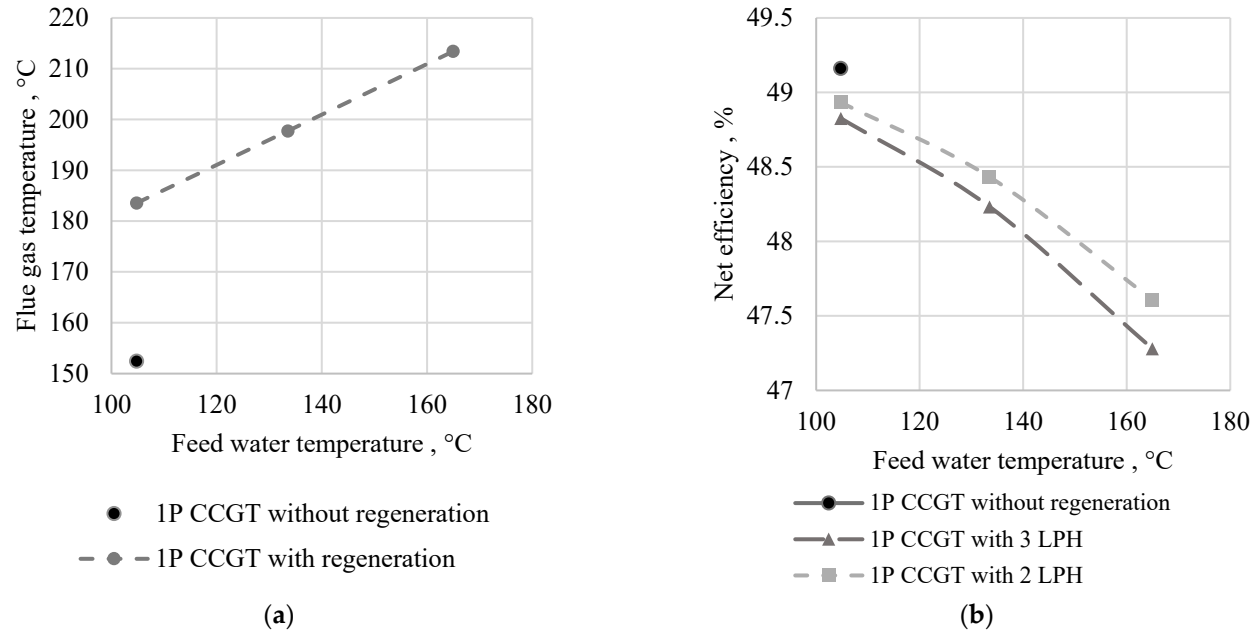

Figure 15. *Cont.*

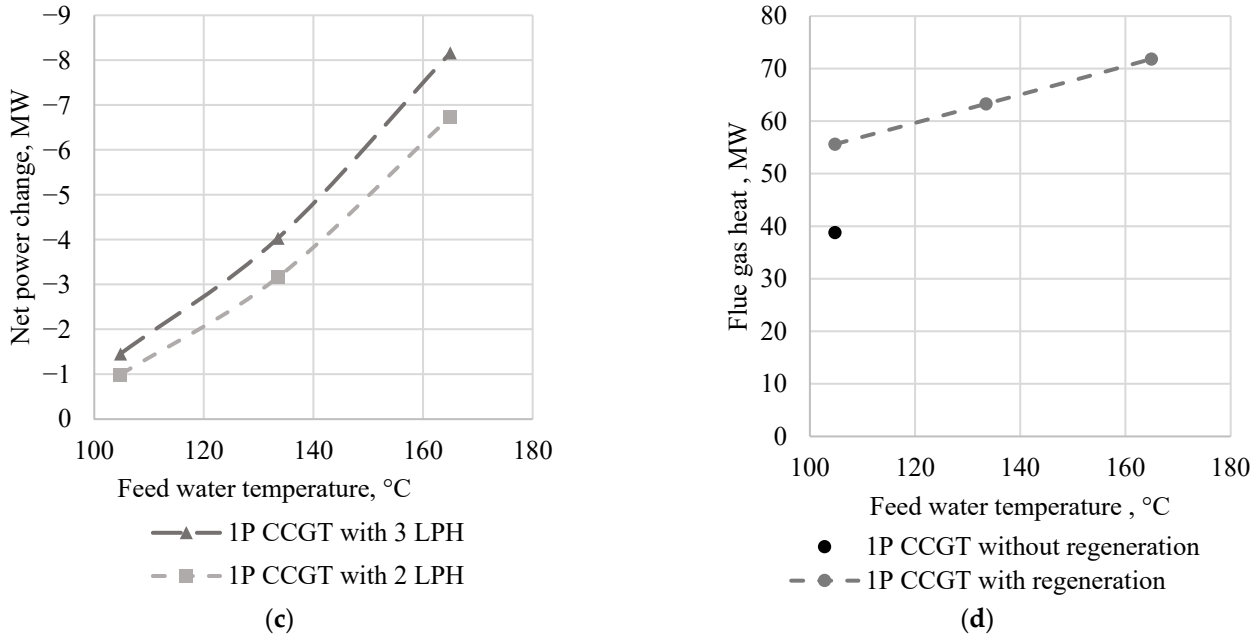

Figure 15. Influence of feed water temperature upon the CCGT characteristics: (**a**) the flue gas temperature, (**b**) net efficiency, (**c**) net power change, (**d**) flue gas heat potential when cooled to 80 °C.

Figure 15b shows a dependence of the CCGT net efficiency on the feed water temperature. The facility with a low-pressure regenerative system has a 0.2–2% lower net efficiency than that with a water heater. When the regeneration system is applied, the HRSG steam production stays constant because of the constant temperature differences in superheater and evaporator. On the other side, the regeneration reduces the STU specific heat drop which reduces its power output. At a higher feed water temperature, the steam parameters in STU bleeding increase, which also reduces the heat drop. Therefore, the use of regeneration systems and increase of the feed water temperature reduce the net efficiency.

Introduction of an STU regeneration system reduces efficiency and power of binary power plants. On the contrary, its use in a trinary facility may produce positive effects that are due to the lower condenser heat losses and higher ORC power and efficiency caused by the higher temperature of HRSG flue gas. Therefore, the implementation assessment must be based on the power output reduction and the low potential heat increase. This is described by the dependence of CCGT net power on the feed water temperature in a single-pressure CCGT without regeneration (Figure 15c). The regeneration reduces the power output by 1–8 MW depending upon the deaerator pressure. The flue gas heat increases by 15 MW at the feed water temperature about 105 °C and by 33 MW at 165 °C (Figure 15d).

Further analysis is carried out for two basic plants. In the first power unit, the ORC is used for heat utilization after a single-pressure CCGT without regeneration and with exit gas temperature of about 152 °C. In this case, it is possible to modify existing single-pressure units without main equipment changes.

In the second case, the flue gas of single-pressure CCGT with regeneration, 2 LPHs, and feed water of 105 °C is utilized. In this case, the exhaust gas temperature is about 184 °C. This power unit allows a remarkable increase of the flue gas temperature and heat without a remarkable reduction of the CCGT net power.

3.3. Organic Rankine Cycles for Waste Heat Utilization

Figure 16 shows the ORC power when utilizing the flue gas heat. In all cases, the net power without regeneration is smaller, while the cycles with regeneration have lower optimal pressures. This is due to the fact that with a decrease in the initial pressure, the

temperature at the turbine exhaust increases, which increases the available temperature difference in the regenerator and makes it possible to increase the temperature of the working fluid at the heater inlet. This, in turn, makes it possible to increase the parameters of the working fluid at the turbine inlet and increase the generated power. Distribution of the ORC power for most of the working fluids repeats the critical temperatures distribution. In the case of heat utilization with R236ea, in the first case, the further initial pressure increase leads to an excess of humidity at the outlet of the turbine.

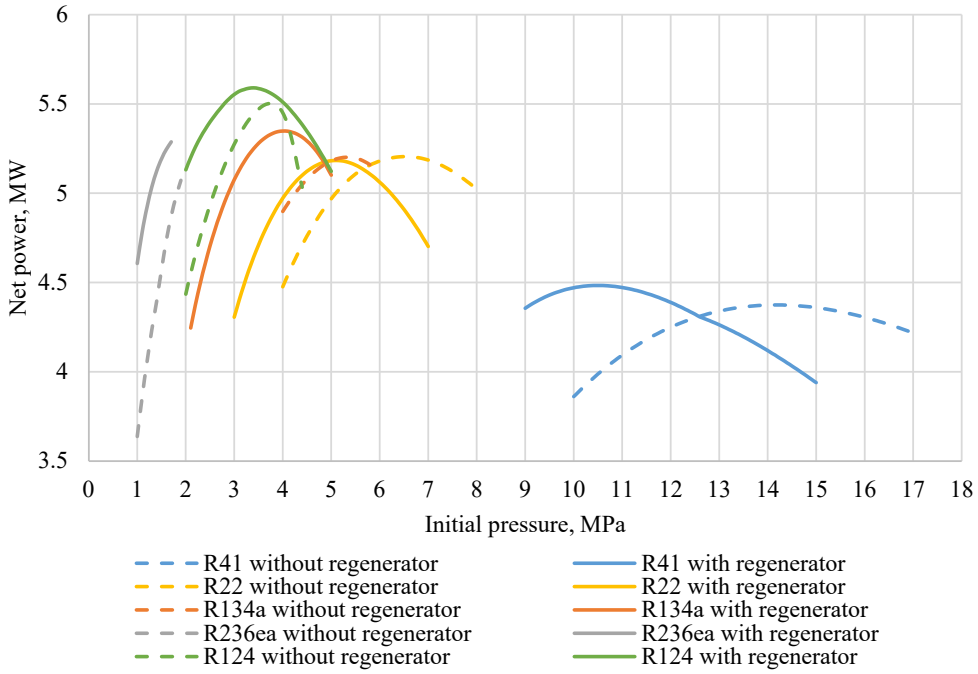

(**a**)

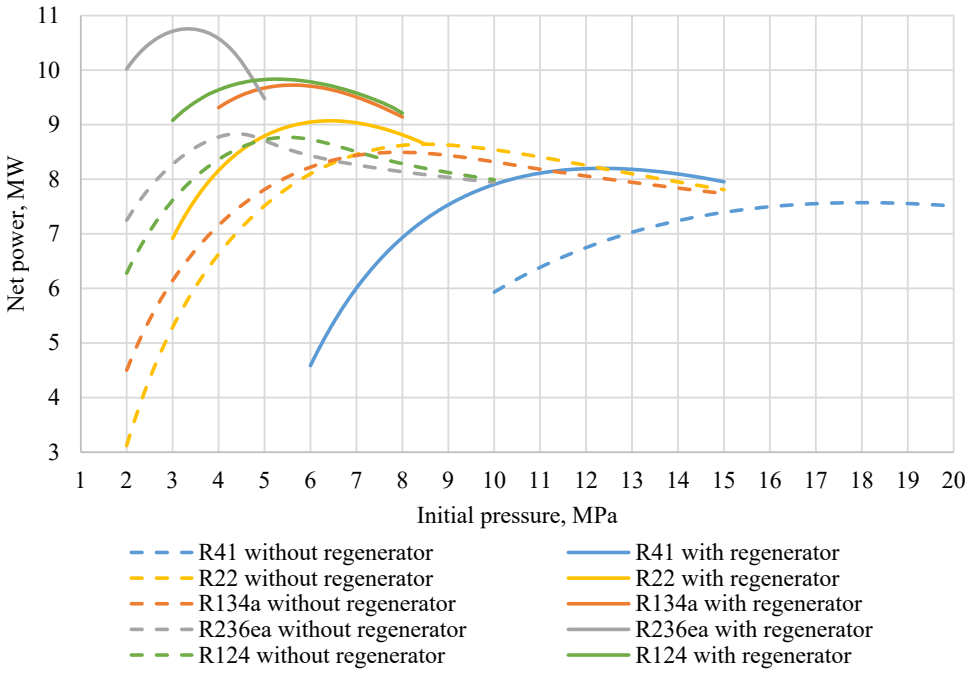

(**b**)

Figure 16. ORC net power with different hot sources: (**a**) flow after a single-pressure CCGT; (**b**) flow after a single-pressure CCGT with regeneration and the feeding water temperature of 105 °C.

The most effective ORC for utilizing heat after the single-pressure CCGT is the one working with R124 and a regenerator at initial pressure of 3.4 MPa, which makes it possible to have a low-potential cycle power of 5.59 MW. For the flow with 180 °C temperature, the most effective is the cycle with regeneration using the R236ea and initial pressure of 3.3 MPa. In this case, the low potential cycle net power is 10.76 MW.

Therefore, when using regeneration in STU, it is reasonable to use the ORC with regeneration and R236ea. When utilizing the heat of flue gases after single-pressure CCGT without regeneration, one should use the ORC with regeneration and R124.

3.4. Trinary Cycles

Table 7 represents the calculation results for trinary cycles with ORC for utilization of flue gas heat after the CCGT with and without regeneration in STU and feeding water of 105, 134, and 165 °C. In every point, the low-potential cycle initial pressure was optimized.

Table 7. Trinary cycle parameters with CCGT.

Regeneration	Without Regeneration	With Regeneration		
Feed water temperature, °C	104.78	104.78	133.52	164.95
Fuel flow, kg/s	8.68	8.68	8.68	8.68
GT net power, MW	143.50	143.50	143.50	143.50
STU net power, MW	69.85	68.40	65.82	61.69
ORC net power, MW	5.59	10.76	12.04	14.52
Trinary cycle net power, MW	218.95	222.66	221.37	219.71
Single-pressure CCGT net efficiency, %	49.16	48.83	48.23	47.28
Trinary cycle efficiency, %	50.45	51.30	51.01	50.63
Dual-pressure CCGT net efficiency, %	50.86	50.86	50.65	50.25

Figure 17 shows dependencies of power and efficiency upon the feed water temperature. Application of the regeneration increases the facility efficiency. Increase of the feed water temperature reduces the unit power and efficiency. The water temperature increase from 105 to 165 °C is followed by the trinary facility net power drop from 222.7 to 219.7 MW. In all versions, the dual-pressure CCGT has lower net efficiency than the trinary power unit (Figure 17b).

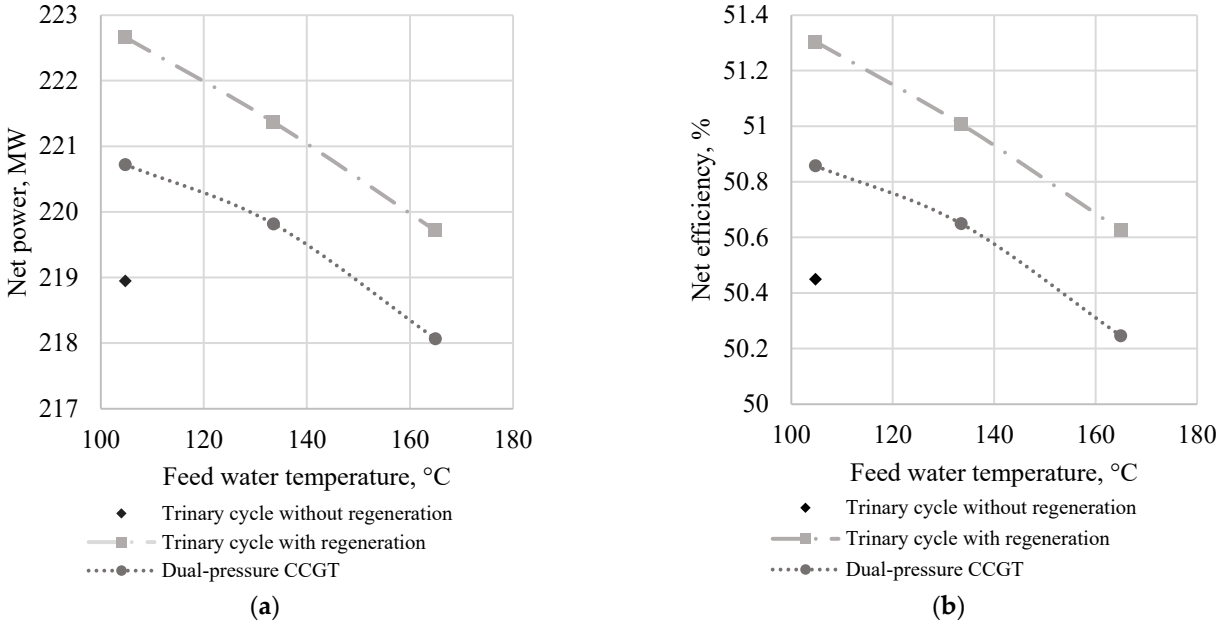

Figure 17. Net power and efficiency of trinary cycles at different feeding water temperatures: (**a**) net power, (**b**) net efficiency.

Figure 18 compares net power and efficiency of trinary power units with different configurations. The trinary cycle with regeneration has maximal efficiency of 51.3% at the feed water temperature of 105 °C. Use of the flue gas heat from a single-pressure CCGT in ORC produces the net power increase of 5.59 MW. Due to the introduction of regeneration into an STU, the trinary cycle net power increases by 3.71 MW and reaches 222.6 MW. The power and efficiency increase due to the shift to the trinary cycle is 1.5 times larger than the increase from the STU regeneration introduction.

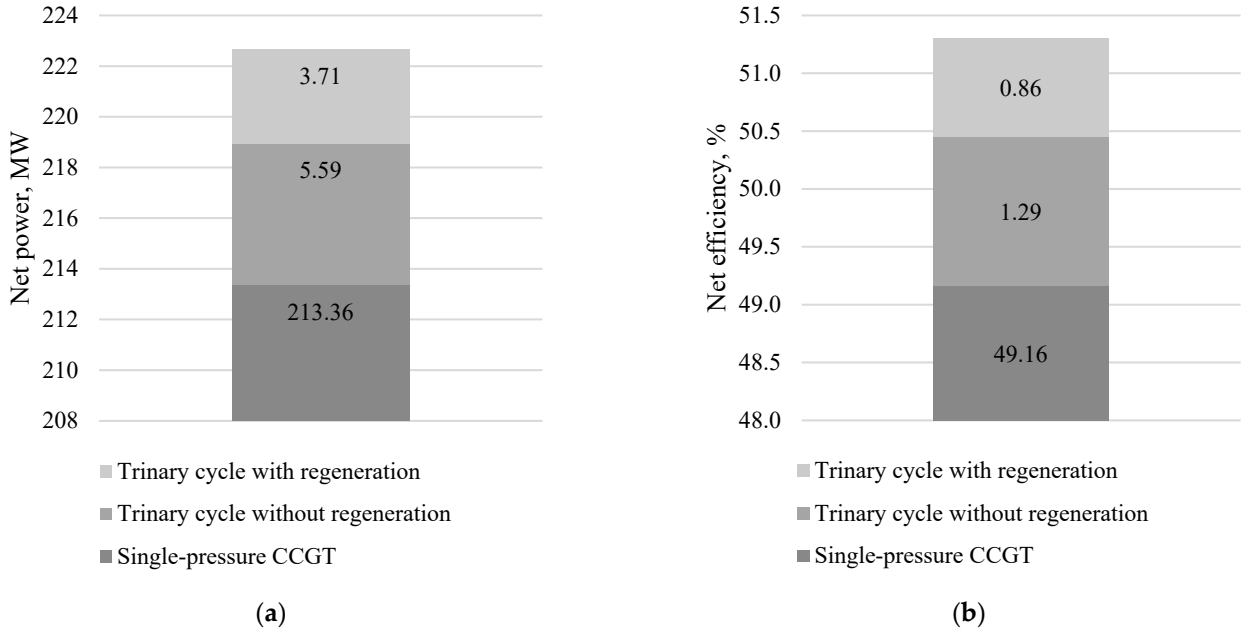

Figure 18. The effect of transition from single-pressure CCGT to trinary cycle: (**a**) net power, (**b**) net efficiency.

The assessment of the impact of the transition to trinary cycles can be made on the basis of an analysis of the increase in installed capacity. This method is approximate, since different CCGTs are located in different climatic zones with different average annual air temperatures, which significantly affects the efficiency, power, and temperature of the gas turbine exhaust gases. In addition, different units may have different configurations of HRSG. Thus, the transition to the trinary cycles will lead to the increase of installed CCGT with GTE-160 in Russia by 52–262 MW depending on the unit composition.

3.5. Economic Assessment

To calculate the economic parameters of trinary power plant operation, an assessment was made using a low-potential cycle for utilizing the heat of exhaust gases from a single-pressure CCGT without regeneration. In this case, the additional power production due to transition to the trinary cycle is equal to 5.59 MW. The main expenses are the purchase of equipment and repairs and maintenance. A source of profit is the sale of additional electrical energy on the wholesale market.

Capital costs for ORC projects vary, but for similar conditions, they are estimated to be 1000–3000 EUR_{2014}/kW [41]. The initial data for the calculation were taken according to Table 8. The electricity cost growth rates were taken from the PJSC Mosenergo forecast and are in the range of 1.3–4.7%. The capacity payments for 10 years were assumed to be 1000 RUB/MW·month due to the capacity supply contracts for power stations modernization in Russia. After 10 years, the period capacity payments were based on the predicted market values. The startup date was assumed to be 2020 and all costs were converted to this date.

Table 8. Economic analysis input data.

Parameter	Value	Source
ORC capital cost, USD_{2012}/kW	1580	[42]
O&M cost, %	3	[43]
Capacity utilization factor	0.7	-
Expected lifetime, h	200,000	-
Discount rate, %	12	-
Income tax, %	20	-
Exchange rate, RUB/USD	57	[44]
Electricity cost, RUB_{2020}/MWh	1320	[45]

The net present value (NPV) was calculated to be equal to 37,780 USD with the discounted payback period (DPP) of 18 years (Figure 19).

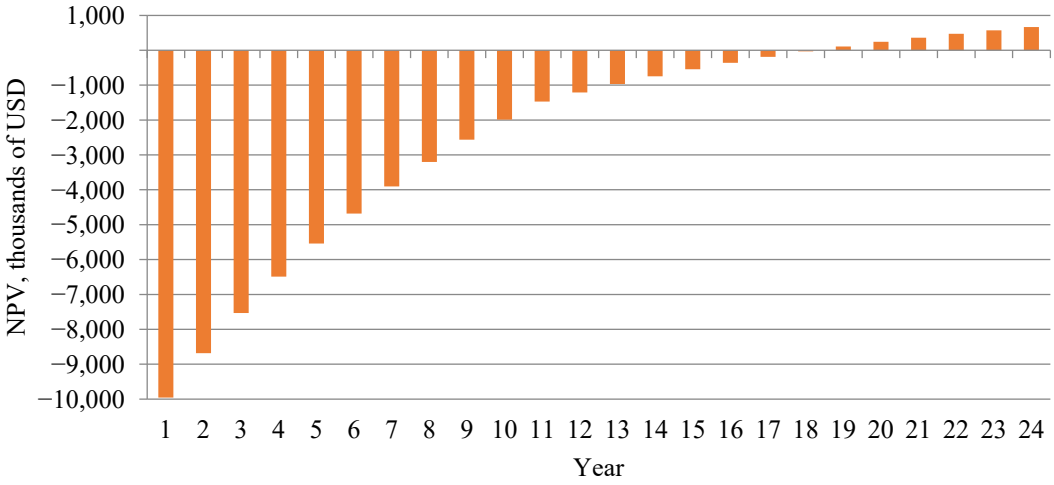

Figure 19. Net present value of the project through years.

Results of sensitivity analysis are presented in Figure 20. The largest influence on NPV hass the capital cost of ORC equipment, followed by discount rate and electricity cost. The same can be seen for the discounted payback period. In the cases when the variation is lower than −100%, the project becomes unprofitable and the payback period was not calculated.

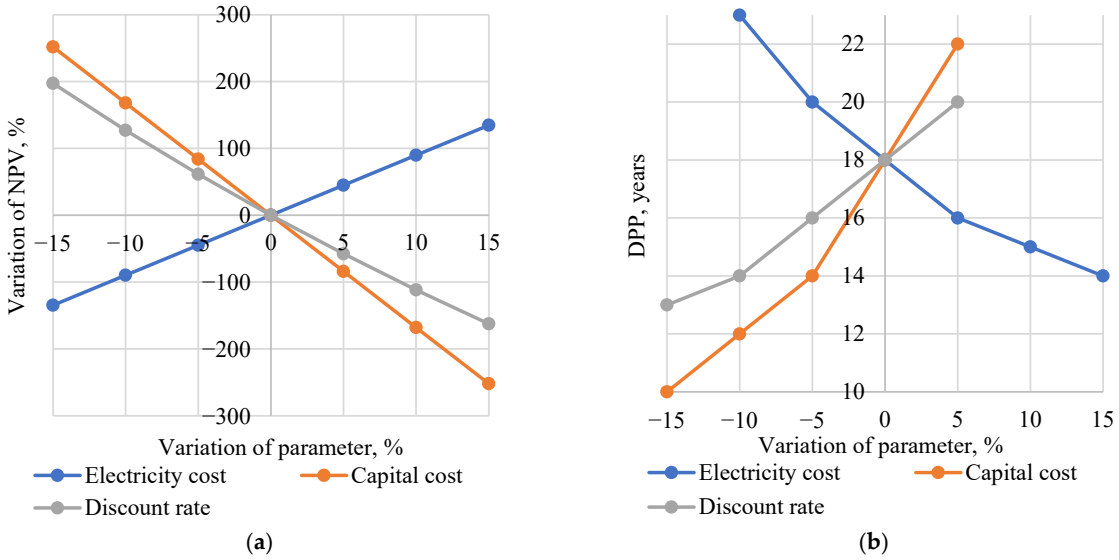

Figure 20. Parameters effect on the projects: (**a**) NPV, (**b**) DPP.

4. Conclusions

1. The developed mathematical model of a cooled gas turbine is based on existing GT facilities characteristics using the NIST REFPROP database and the Aspen Plus computer program. The model allows for assessment of coolant flow, GT compressor, and turbine power and the exhaust gas characteristics at different initial parameters and ambient air conditions.
2. At the heat source temperature of about 152 °C, the maximum net power of the Organic Rankine cycle is reached with the R124 heat carrier. At the heat source temperature above 184 °C, the maximum electric power of the Organic Rankine cycle is reached with the R236ea heat carrier. This due to the R236ea higher critical parameters, which allow for lower turbine inlet pressure and smaller pump power.
3. At the heat source temperature of 152 °C, application of regeneration in ORC provides an electric power output increase of 1.6–4.2% and 5–21.8% for 184 °C.
4. The trinary power cycle reaches its maximum net efficiency and power at the deaerator pressure of 0.12 MPa, which corresponds with the feed water temperature of 105 °C and ORC with regeneration and R36ea.
5. Due to the heat utilization of a single-pressure CCGT flue gas by ORC, the net power and efficiency increases from 213.36 to 218.96 MW and from 49.16% to 50.45%, respectively. Introduction of the low-pressure regeneration in STU increases the trinary cycle net power and efficiency up to 222.66 MW and 51.30%, respectively. Thus, the trinary power plant with regeneration has net efficiency of 2.14% and 0.36–0.45% higher than the single- and dual-pressure CCGT, respectively. The transition from binary to trinary cycles using GTE-160 in Russia will lead to the 52–262 MW increase in the installed capacity.
6. The economic analysis shows that the use of ORC for utilization of gas heat after single-pressure CCGT is viable and has the NPV of 37,780 USD with DPP of 18 years. The largest influence on the economic effect is caused by the capital cost of ORC, followed by discount rate and electricity cost.

Author Contributions: Conceptualization, V.K.; methodology, N.R.; software, V.N.; validation, S.O.; formal analysis, O.Z.; investigation, V.N. and S.O.; resources, N.R.; data curation, O.Z.; writing—original draft preparation, V.N.; writing—review and editing, N.R.; visualization, S.O.; supervision, V.K.; project administration, V.K.; funding acquisition, O.Z. All authors have read and agreed to the published version of the manuscript.

Funding: This study was conducted by National Research University "Moscow Power Engineering Institute" and was supported by the Russian Science Foundation under Agreement No. 21-79-00262 dated by 27 July 2021.

Institutional Review Board Statement: Not applicable.

Informed Consent Statement: Not applicable.

Data Availability Statement: Not applicable.

Conflicts of Interest: The funders had no role in the design of the study; in the collection, analyses, or interpretation of data; in the writing of the manuscript, or in the decision to publish the results.

References

1. IEA. *Global Energy Review 2019*; IEA: Paris, France, 2020.
2. Singh, S. Energy Crisis and Climate Change: Global Concerns and Their Solutions. In *Energy*; Wiley: Hoboken, NJ, USA, 2021; Volume 1, pp. 1–17. [CrossRef]
3. Chofreh, A.G.; Goni, F.A.; Klemeš, J.J.; Moosavi, S.M.S.; Davoudi, M.; Zeinalnezhad, M. COVID-19 Shock: Development of Strategic Management Framework for Global Energy. *Renew. Sustain. Energy Rev.* **2021**, *139*, 110643. [CrossRef]
4. Chen, W.-H.; Ong, H.C.; Ho, S.-H.; Show, P.L. Green Energy Technology. *Energies* **2021**, *14*, 6842. [CrossRef]
5. Jabeen, G.; Ahmad, M.; Zhang, Q. Factors Influencing Consumers' Willingness to Buy Green Energy Technologies in a Green Perceived Value Framework. *Energy Sources Part B Econ. Plan. Policy* **2021**, *16*, 669–685. [CrossRef]

6. Wang, C.-H.; Zhao, D.; Tsutsumi, A.; You, S. Sustainable Energy Technologies for Energy Saving and Carbon Emission Reduction. *Appl. Energy* **2017**, *194*, 223–224. [CrossRef]
7. Chowdhury, J.I.; Hu, Y.; Haltas, I.; Balta-Ozkan, N.; Matthewb, G.J.; Varga, L. Reducing Industrial Energy Demand in the UK: A Review of Energy Efficiency Technologies and Energy Saving Potential in Selected Sectors. *Renew. Sustain. Energy Rev.* **2018**, *94*, 1153–1178. [CrossRef]
8. Rogalev, A.; Rogalev, N.; Kindra, V.; Komarov, I.; Zlyvko, O. Research and Development of the Oxy-Fuel Combustion Power Cycles with CO2 Recirculation. *Energies* **2021**, *14*, 2927. [CrossRef]
9. Kindra, V.; Rogalev, A.; Lisin, E.; Osipov, S.; Zlyvko, O. Techno-Economic Analysis of the Oxy-Fuel Combustion Power Cycles with Near-Zero Emissions. *Energies* **2021**, *14*, 5358. [CrossRef]
10. Morimoto, K.; Matsumura, Y.; Suzuki, K.; Wakazono, S.; Kataoka, M.; Yuri, M. Operation Status of 1650 °C Class M501JAC Gas Turbine at T-Point 2 Power Plant Demonstration Facility. *Mitsubishi Heavy Ind. Tech. Rev.* **2021**, *58*, 10.
11. Ol'khovskii, G.G. The Most Powerful Power-Generating GTUs (A Review). *Therm. Eng.* **2021**, *68*, 490–495. [CrossRef]
12. Morimoto, K.; Matsumura, Y.; Iijima, T.; Wakazono, S.; Kataoka, M.; Yuri, M. Validation Results of 1650 °C Class JAC Gas Turbine at T-Point 2 Demonstration Plant. *Mitsubishi Heavy Ind. Tech. Rev.* **2021**, *58*, 12.
13. Okajima, Y.; Torigoe, T.; Mega, M.; Kuwabara, M.; Okaya, N. Development of Advanced TBC for 1650 °C Class Gas Turbine. In Proceedings of the ITSC2021, Indianapolis, IN, USA, 19–22 September 2021; pp. 695–699.
14. Zaryankin, A.; Mager, A.; Rogalev, A.; Komarov, I. Superpowerful Combined Cycle Power Units with One Gas Turbine. *WIT Trans. Ecol. Environ.* **2014**, *190*, 10.
15. Mitsubishi. *GTCC Gas Turbine Combined Cycle Power Plants*; Mitsubishi Heavy Industries: Kanagawa, Japan, 2021; p. 12.
16. Bassily, A. Enhancing the Efficiency and Power of the Triple-Pressure Reheat Combined Cycle by Means of Gas Reheat, Gas Recuperation, and Reduction of the Irreversibility in the Heat Recovery Steam Generator. *Appl. Energy* **2008**, *85*, 1141–1162. [CrossRef]
17. Bassily, A. Modeling, Numerical Optimization, and Irreversibility Reduction of a Dual-Pressure Reheat Combined-Cycle. *Appl. Energy* **2005**, *81*, 127–151. [CrossRef]
18. Kwon, H.M.; Moon, S.W.; Kim, T.S.; Kang, D.W. Performance Enhancement of the Gas Turbine Combined Cycle by Simultaneous Reheating, Recuperation, and Coolant Inter-Cooling. *Energy* **2020**, *207*, 118271. [CrossRef]
19. Grinchuk, A. Improving the Efficiency of Waste CCGTs Through the Application of Intermediate Steam Reheating. *Energy News High. Educ. Inst. Energy Assoc. CIS* **2008**, *5*, 78–86.
20. Elmasri, M. Triple-Pressure and Reheat Combined Cycles: Design-Point Thermodynamics. In *Design of Gas Turbine Combined Cycles and Cogeneration Systems*; Thermoflow: Jacksonville, FL, USA, 2007; Volume 12.1.
21. Tajik Mansouri, M.; Ahmadi, P.; Ganjeh Kaviri, A.; Jaafar, M.N.M. Exergetic and Economic Evaluation of the Effect of HRSG Configurations on the Performance of Combined Cycle Power Plants. *Energy Convers. Manag.* **2012**, *58*, 47–58. [CrossRef]
22. Hada, S.; Yuri, M.; Masada, J.; Ito, E.; Tsukagoshi, K. Evolution and future trend of large frame gas turbines: A new 1600 degree c, j class gas turbine. In *Turbo Expo: Power for Land, Sea, and Air*; American Society of Mechanical Engineers: Copenhagen, Denmark, 2012; pp. 599–606.
23. Rogalev, A.; Rogalev, N.; Kindra, V.; Zlyvko, O.; Vegera, A. A Study of Low-Potential Heat Utilization Methods for Oxy-Fuel Combustion Power Cycles. *Energies* **2021**, *14*, 3364. [CrossRef]
24. Rogalev, N.; Kindra, V.; Komarov, I.; Osipov, S.; Zlyvko, O.; Lvov, D. Comparative Analysis of Low-Grade Heat Utilization Methods for Thermal Power Plants with Back-Pressure Steam Turbines. *Energies* **2021**, *14*, 8519. [CrossRef]
25. Galashov, N.; Tsibulskiy, S.; Serova, T. Analysis of the Properties of Working Substances for the Organic Rankine Cycle Based Database "REFPROP". *EPJ Web Conf.* **2016**, *110*, 01068. [CrossRef]
26. Galashov, N.; Tsibulskiy, S. Parametric Analysis of the Diagram of the Combined-Cycle Gas Turbine with a Combination of Three Cycles for Improving Efficiency When Operating in Northern Gas Producing Areas. *Bull. Tomsk. Polytech. Univ.* **2019**, *330*, 44–55.
27. Galashov, N. Analysis of Influence of Steam/Turbine Cycle Basic Parameters on the Efficiency of Triple Combined/Cycle Plants. *Bull. Tomsk. Polytech. Univ.* **2013**, *323*, 15–21.
28. Bălănescu, D.-T.; Homutescu, V.-M. Performance Analysis of a Gas Turbine Combined Cycle Power Plant with Waste Heat Recovery in Organic Rankine Cycle. *Procedia Manuf.* **2019**, *32*, 520–528. [CrossRef]
29. Gafurov, A.; Uskov, D.; Shubina, A. Power Plant Based on GTU NK-37 with Two Heat Recovery Working Circuits. *Energy Tatarstan* **2012**, *3*, 35–41.
30. Tugov, A.; Maidanik, M. Steam recovery boilers behind gas turbines with a capacity of more than 25 MW, installed at thermal power plants in Russia. *Gas Turbine Technol.* **2018**, *3*, 12–15.
31. Trukhniy, A. *Combined-Cycle Plant of Power Stations*; MPEI: Moscow, Russia, 2013.
32. Kindra, V.; Rogalev, N.; Rogalev, A.; Naumov, V.; Sabanova, E. Thermodynamic Optimization of Low-Temperature Cycles for the Power Industry. *Energies* **2022**, *15*, 2979. [CrossRef]
33. Aspen Technology, Inc. Aspen Plus. Available online: https://www.aspentech.com/en/products/engineering/aspen-plus (accessed on 19 July 2021).
34. Lemmon, E.W.; Bell, I.H.; Huber, M.L.; McLinden, M.O. *NIST Standard Reference Database 23: Reference Fluid Thermodynamic and Transport Properties-REFPROP*; Version 10.0, National Institute of Standards and Technology; Standard Reference Data Program: Gaithersburg, MA, USA, 2018.

35. Canière, H.; Willockx, A.; Dick, E.; De Paepe, M. Raising Cycle Efficiency by Intercooling in Air-Cooled Gas Turbines. *Appl. Therm. Eng.* **2006**, *26*, 1780–1787. [CrossRef]
36. Shevchenko, I.V.; Rogalev, A.N.; Shevchenko, M.I.; Strogonova, L.B.; Yaropolov, V.I. Application of Additive Laser Technologies for Full-Scale Modeling in the Design of Cooled Gas Turbine Blades. *Int. J. Mech. Eng. Technol.* **2018**, *9*, 2097–2105.
37. Lebedev, A.; Pavlov, A.Y.; Richter, F.; Adamchuk, A. Experience Gained from Operation of the GTE-160 Gas Turbine Installation and Prospects for Its Modernization. *Therm. Eng.* **2013**, *60*, 89–91. [CrossRef]
38. Mikhailov, V.; Khomenok, L.; Zolotogorov, M.; Gasol, M.; Ivanov, A.; Romanov, V.; Skirta, S. Testing Blade Systems of First Stage of Turbine Unit GTE-110 for Improving Its Operational Reliability. *Saf. Reliab. Power Ind.* **2017**, *1*, 190–196. [CrossRef]
39. SZTU Main Technical Characteristics of GTU. Available online: https://vunivere.ru/work33768/page29 (accessed on 16 February 2022).
40. Khusainov, K.; Kudinov, A. Increasing the Efficiency of PGU-450 at Severo-Zapadnaya CHPP in St. Petersburg by Steam Reheating in the Air Cooler of the GTU Turbocompressor. *Reliab. Secur. Energy* **2017**, *2*, 58–64.
41. Lemmens, S. Cost Engineering Techniques and Their Applicability for Cost Estimation of Organic Rankine Cycle Systems. *Energies* **2016**, *9*, 485. [CrossRef]
42. Tartière, T.; Astolfi, M. A World Overview of the Organic Rankine Cycle Market. *Energy Procedia* **2017**, *129*, 2–9. [CrossRef]
43. Elson, A.; Tidball, R.; Hampson, A. *Waste Heat to Power Market Assessment*; ICF International: Fairfax, VA, USA, 2015; p. 86.
44. Official Currency Rates for A Given Date, Set Daily | Bank of Russia. Available online: https://www.cbr.ru/currency_base/daily/ (accessed on 24 February 2021).
45. Association "NP Market Council". *Forecast of Price Indices of the RSV For Sale*; Association "NP Market Council": Moscow, Russia, 2019; p. 29.